

Research Note

Planetary nebula K1-9

L. N. Kondratyeva and E. K. Denissyuk

Fessenkov Astrophysical Institute, Kazakhstan
Isaac Newton Institute of Chile, Kazakhstan Branch

Received 29 January 2002 / Accepted 11 September 2003

Abstract. The object K1-9 with strong [N II] emission lines was included in the Perek and Kohoutek Catalogue of Planetary Nebulae, but later it was considered to be an H II region. Our results show that in addition to the low-excitation emissions there are He II and [O III] emission lines in its spectrum, and the effective temperature of the central star is more than 54 000 K. Thus we conclude that K1-9 is indeed a planetary nebula. Distribution of [O III] and [N II] emission lines reflect a ring-like structure with a clear minimum in the centre of the nebula. Hydrogen lines almost fail to show the central gap. K1-9 has the backward proper motion with systemic velocity $RV = 60.2 \text{ km s}^{-1}$. The central hydrogen component moves relative to the nebula with a peculiar velocity of about -50 km s^{-1} .

Key words. planetary nebulae: general – planetary nebulae: individual: K1-9

1. Introduction

Object K1-9 (PK 219+01:1 = SCM18 = PN ARO228 = PN K1-9) with coordinates (2000): $7^{\text{h}}07^{\text{m}}15^{\text{s}}.6 -5^{\circ}09'58''$ was discovered by Kohoutek (1964), and was listed in the Catalogue of Galactic Planetary Nebulae of Perek & Kohoutek (1967).

A “red light” image of the object from the Palomar Survey has an elliptic ring-like shape with the dimensions of $28'' \times 48''$ (Schwarz et al. 1992), and the “blue light” image is star-like. The magnitude of the central star was first determined by Kohoutek (1964): $p = 18^{\text{m}}.6$ and $r = 18^{\text{m}}.0$, and later the values $B = 19^{\text{m}}.5$ and $V = 19^{\text{m}}.1$ were presented by Kaler et al. (1990). Relative intensities of emission lines and the absolute $H\beta$ flux were measured by Kaler et al. (1990). K1-9 was included in the spectrophotometric survey of Stenholm & Acker at ESO. They obtained two 10 min exposure spectra, showing only faint [N II] and $H\alpha$ lines. As the typical [O III] lines were absent, the object was removed from the true planetary nebulae class (see Acker et al. 1992, p. 2 and Table 2). Our paper presents results of a new detailed spectral study of the ionization structure of K1-9.

2. Observations

Optical observations of the object were acquired from 1986 through 2001 using the slit spectrograph mounted at the Cassegrain focus of the 70 cm telescope at the Observatory of the Fessenkov Astrophysical Institute (Almaty, Kazakhstan). This device is fully described by Denissyuk (2003). The three-stage image tube was used as a detector until 1998, and a

ST7 CCD since 1999. Two gratings (1200 lines mm^{-1} and 600 lines mm^{-1}) were used. Two camera lenses ($F = 250 \text{ mm}$ and $F = 150 \text{ mm}$) provided the spectral regions: $\lambda\lambda 3700\text{--}5800 \text{ \AA}$ and $\lambda\lambda 5700\text{--}8600 \text{ \AA}$.

In the first variant, with the image tube, spectrograms were obtained with reciprocal dispersion in the range $25\text{--}100 \text{ \AA mm}^{-1}$ with a spectral resolution from 0.8 up to 3 \AA with the adopted slit width of $4''$. The spectra of some bright, well studied planetary nebulae, such as NGC 7027, NGC 7662, NGC 2022 (Peimbert et al. 1987; Keyes et al. 1990), were used in order to correct the S-distortion, inherent to the image tube, and to level out the wavelength dependence of the instrumental response. The precision of intensities is about 10–15% for moderate and strong emission lines. The errors of faint line measurements may be as high as 50% or even more.

In the second variant, with the ST7 CCD ($765 \times 510, 9 \mu\text{m}$), spectrograms with dispersions of 1.1 and 0.5 \AA pix^{-1} with a resolution of 2.5 and 1.0 \AA (with the adopted slit width of $2''$) were obtained. The spectra were reduced following the usual steps (dark and flat-field corrections).

In both variants of the device the exposure times were adjusted between 40 and 60 min. No absolute flux calibration was attempted. Spectrograms of the object were sky subtracted, and wavelength calibration through a He-Ar-Ne lamp was performed. In order to demonstrate the reliability of our observations the comparison of our results with other authors for 15 planetary nebulae is presented (Fig. 1).

The Y -axis shows values of $\Delta = (I_{\text{ours}} - I_{\text{other}})/I_{\text{other}}$ in percent. Data for Cn3-1, Hu1-1, K3-61, M1-5, M1-11, M1-12, M1-14, M1-16, M1-17, M1-61, M2-50, M3-35, PC12 and Sn1 from (Barker 1978; Cuisiner et al. 1996; Acker et al. 1992;

Send offprint requests to: L. Kondratyeva,
e-mail: kon@.afi.south-capital.kz

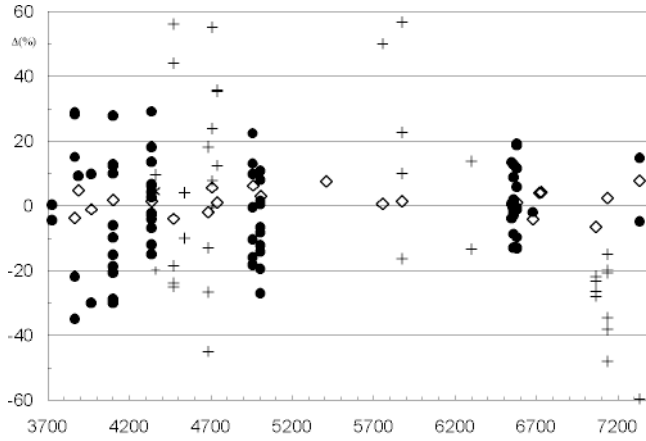


Fig. 1. Comparison of our results with other authors.

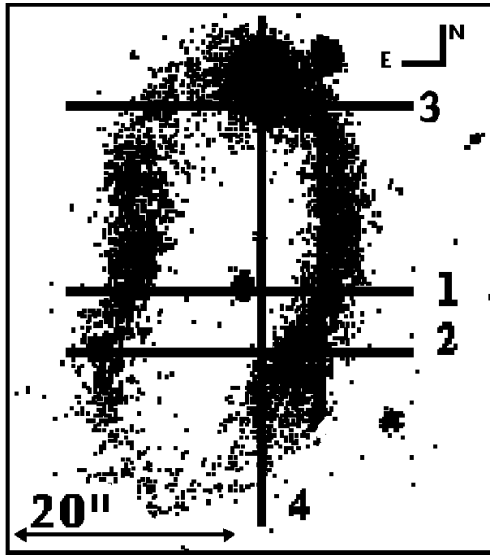


Fig. 2. A “red light” image of K1-9. Black lines show the slit positions.

Costa et al. 1996; Aller et al. 1979, 1987; Peimbert et al. 1987) were used. Our results were obtained with the image tube, references may be found in the Catalogue (Acker et al. 1992). It is seen that data for the strong and moderate lines (filled circles) are displayed within the range $\pm 20\%$. The faint lines with $I(\lambda) \leq 0.15I(\text{H}\beta)$, denoted by crosses, have much more dispersion. Observations of NGC 7027 were carried out with the ST7 CCD, they are presented in Fig. 1.

3. Results

Altogether 12 spectrograms of K1-9 with moderate dispersion were selected for the following photometric treatment (5 – in the blue spectral range and 7 – in the red). All of them but one were obtained with the image tube. Six additional spectra with a dispersion of 25 \AA mm^{-1} in $\text{H}\alpha$ were obtained with the image tube specially for the study of profiles and shifts of lines. Observations with a CCD in 2001 were also used for measurements of RV .

In order to study different regions of the nebula, the slit of the spectrograph was placed in four positions, three east-west

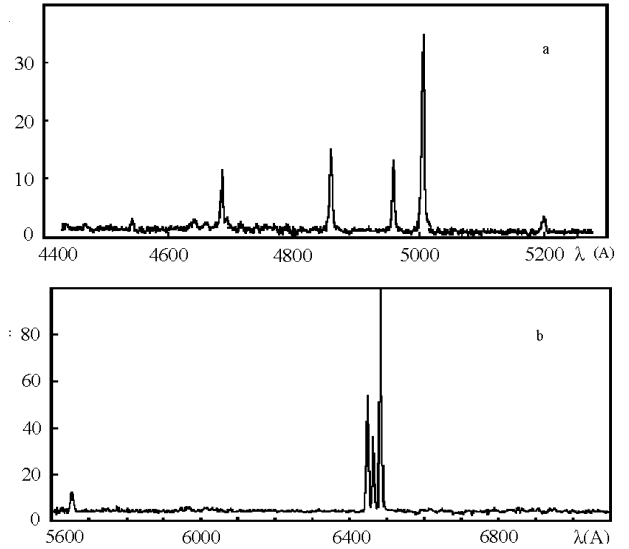


Fig. 3. Blue and red spectra of K1-9 integrated over slit 1.

and one north-south. Figure 2 shows the slit positions superimposed on the “red image”, of the object, taken from the paper of Schwarz et al. (1992). Relative intensities were obtained for all observed lines. The extinction constant $C(\text{H}\beta) = 0.60 \pm 0.06$ was found from $I(\text{H}\alpha)$ to $I(\text{H}\beta)$ intensities ratio. This value is similar to the result of Kaler et al. (1990).

An emission spectrum of K1-9, integrated over slit 1, is presented in Figs. 3a,b. The Y -axis shows the relative intensities, expressed in the scale $I_{\lambda=4861} = 1$.

Spectrograms obtained with a dispersion of 60 \AA mm^{-1} in 1989 and 1996 were combined to make the spectrum in the wavelength range $\lambda\lambda 3700\text{--}5300 \text{ \AA}$ (Fig. 3a). Results obtained in 1998 with the image tube and CCD spectrograms of 2001 were averaged to construct the “red” spectrum (Fig. 3b). Relative intensities of emission lines derived from observations in 1991–1998 are presented in Table 1. Integrated over the whole slit, values are dereddened and expressed in the scale $I(\text{H}\beta) = 100$.

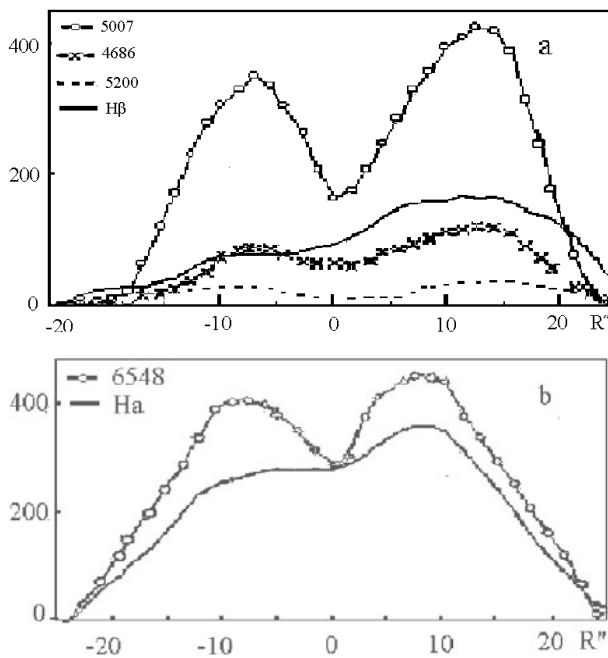
To exclude suspicions about any systematic errors of our results connected with observations or reductions, we present the observed line intensities of another extended object Sh1-89, comparing with the data of Kaler et al. (1990). Both rows, given in Cols. 7 and 8 of Table 1, are related to the central region of the nebula. For all but two lines ($[\text{N I}]$, $[\text{O I}]$), the difference between two determinations is no more than 10%, and no systematic errors are revealed. A similar conclusion may be drawn from an analysis of Fig. 1: no systematic errors are noted along the wide wavelength range. Thus our results for K1-9 may be considered as reliable.

Because of limited observational data an empirical method for determination of the central star’s temperature was applied. The relation between T^* and maximum observed ionization energy χ (eV) from Murset et al. (1994) was used. For $\chi = 54.4 \text{ eV}$ $T^* = 54\,400 \text{ K}$ was derived.

The distributions of line intensities along the central slit position are presented in Fig. 4. The X -axis shows the relative distance from the central star (in arcsec). The intensity of $\text{H}\beta$ near the central star has been accepted to be equal to 100. The

Table 1. Relative intensities of emission lines in the spectra of K1-9 and Sh1-89.

Line(λ)	Element	Spectrum of K1-9				Spectrum of Sh1-89	
		Dereddened intensities relative to $H\beta = 100$				Measured intensities relative to $H\beta = 100$	
		slit 1	slit 2	slit 3	slit 4	Our data	Kaler
4686	He II	76	72	54	63	38	39
4861	$H\beta$	100	100	100	100	100	100
4959	[O III]	85	88	100	91	220	175
5007	[O III]	238	240	288	270	640	737
5200	[N I]	20	16	18	17	15.4	12
6548	[N II]	419	337	390	350	389	394
6563	$H\alpha$	288	287	288	289	520	550
6583	[N II]	1220	950	1130	1200	1175	1271

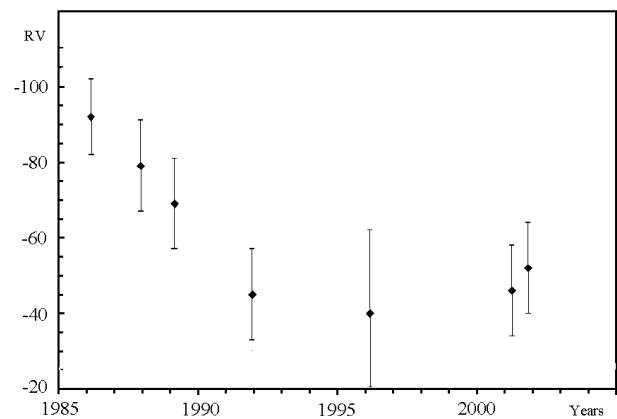
**Fig. 4.** Distributions of emission lines intensities along the central slit position.

distributions of the [N II] and [O III] emissions are quite similar and reflect the ring-like structure. The central gap appears less pronounced for other elements, especially for hydrogen.

It is appears that the central part of the nebula is filled with hydrogen but is almost free of the other elements.

Almost all emission lines in the spectrum of K1-9 are redshifted. Table 2 presents heliocentric radial velocities, derived from measurements for three slit positions and for several dates of observations. [O III] and [N II] lines were measured in the northern ring (slit 3 and 4) and in the eastern + western (slit 1). Shifts of hydrogen lines for slit 1 were measured only in the centre, and in the case of slit 3 – only in the ring. For slit 4 radial velocities of hydrogen were determined in the direction of the centre and in the northern ring. Relevant data in Table 2 (6, 7 columns) are denoted by letters “c” (centre) and “r” (ring).

The last line of Table 2 shows that the average values obtained for each slit position are similar and lead to a mean radial velocity of $60.2 \pm 2.3 \text{ km s}^{-1}$. As it is seen from the 7th and 11th columns, the central $H\alpha$ shows the wide scatter of

**Fig. 5.** Velocity variations of the central hydrogen component relative to the nebula.

heliocentric radial velocities: from -36 km s^{-1} in 1986 up to $+15 \text{ km s}^{-1}$ in 2001. The same tendency is studied in $H\beta$ in spite of the higher errors of its RV. We analyze these data in terms of one-sided flow of the hydrogen component, directed towards the observer. The last column of Table 2 and Fig. 5 contain the radial velocity of this movement relative to the nebula: $RV_{\text{outflow}} = RV(H) - RV_{\text{neb}}$.

4. Discussion and conclusions

Taking into account that the spectrum of K1-9 has a high ionization degree ([O III], He II) and that the effective temperature of its central star $T_{\text{eff}} \geq 54\,000 \text{ K}$, we conclude that this object is a planetary nebula. Due to its shape, radial velocity and T_{eff} , K1-9 corresponds to ellipticals, but its nitrogen abundance is more peculiar for bipolars, moreover – for extreme members of this class with the highest [N II]/ $H\alpha$ ratio (Tajitsu & Tamura 1999).

As it was mentioned above the distribution of hydrogen in the envelope of K1-9 almost does not show the ring-like structure, and $H\text{I}$ emission lines, observed towards the centre, are blue – shifted relative to the other line positions specifying the movement of the hydrogen component towards the observer.

A similar additional faint blue-shifted hydrogen emission with $V = -120 \text{ km s}^{-1}$ was detected in IC 351 (Yadomaru et al. 1992). This reflects one-sided flow with the rear side being obscured or suppressed. In the case of K1-9 the velocity

Table 2. Heliocentric radial velocities in K1-9.

Data	Slit 3		Slit 4				Slit 1				RV_{outflow}
	[N II]	H α	[N II]	[O III]	H β	H α	[N II]	[O III]	H β	H α	
02.1986	61 \pm 6	59 \pm 6	60 \pm 10	44 \pm 20	-29 \pm 20(c) 44 \pm 20(r)	-27 \pm 12(c) 49 \pm 12(r)	62 \pm 6	-	-	-40 \pm 8	-92 \pm 10
12.1987	-	-	-	-	-	-	64 \pm 6	-	-	-19 \pm 10	-79 \pm 12
02.1989	-	-	-	44 \pm 18	50 \pm 20(r)	-	71 \pm 8	56 \pm 15	5 \pm 15	-9 \pm 10	-69 \pm 12
12.1991	64 \pm 7	73 \pm 10	-	-	-	-	66 \pm 6	-	-	15 \pm 10	-45 \pm 12
02.1996	-	-	-	-	-	-	-	62 \pm 20	20 \pm 20	-	-40 \pm 22
12.1998	62 \pm 7	57 \pm 10	-	-	-	-	-	-	-	-	-
03.2001	-	-	-	-	-	-	65 \pm 7	-	-	14 \pm 10	-46 \pm 12
10.2001	-	-	56 \pm 8	-	-	8 \pm 10(c)	-	-	-	-	-52 \pm 12
RV(aver)	62.5 \pm 3.0	63.0 \pm 5.1	58.0 \pm 5.4	44 \pm 11	47 \pm 11(r)	49 \pm 12(r)	65.6 \pm 2.4	59 \pm 10	-	-	

of HI flux decreases over time may be due to interaction with the matter of the main envelope and/or with interstellar matter, its most recent value is about -50 km s^{-1} .

References

- Acker, A., Chopinet, M., Pottasch, C. Q., & Stenholm, B. 1987, A&AS, 71, 163
- Acker, A., & Stenholm, B. 1990, A&AS, 86, 219
- Acker, A., Ochsenbein, F., & Stenholm, B. 1992, The Strasbourg-ESO Catalogue of Galactic Planetary Nebulae (Garching: ESO)
- Aller, L., & Czyzak, S. 1979, ApJS, 62, 397
- Aller, L., & Keyes, C. 1987, ApJS, 65, 405
- Barker, T. 1978, ApJ, 219, 914
- Costa, R. d. D., Chappini, C., Maciel, M. J., & de Freitas Pacheco 1997, A&AS, 116, 249
- Cuisiner, F., Acker, A., & Koppen, J. 1996, A&A, 307, 215
- Denissyuk, E. 2003, A&A Trans., 22, 175
- Kaler, J. B., Shaw, R. A., & Kwitter, K. R. 1990, ApJ, 359, 392
- Keyes, C. D., Aller, L. H., & Peibelman, W. 1990, PASP, 102, 59
- Kohoutek, L. 1964, BAS, 15, 161
- Murset, U., & Nussbaumer, H. 1994, A&A, 282, 586
- Peimbert, M., & Torres-Peimbert, S. 1987, Rev. Mex. Astron. Astrofis., 14, 540
- Perek, L., & Kohoutek, L. 1967, Catalogue of Galactic Planetary Nebulae, Prague, 1967
- Schwarz, H. E., Corradi, L. M. R., & Melnick, J. 1992, A&AS, 96, 23
- Tajitsu, A., & Tamura, S. 1999, PASP, 111, 1157
- Yadomaru, Y., & Tamura, S. 1992, Proc. of the 155th IAU Symp., 379